Journal of Alloys and Compounds 648 (2015) 258–264

Contents lists available at ScienceDirect

Journal of Alloys and Compounds

journal homepage: http://www.elsevier.com/locate/jalcom

Coupling of Hubbard fermions with phonons in La_2CuO_4: A combined study using density-functional theory and the generalized tight-binding method

E.I. Shneyder [a, b, *], J. Spitaler [c], E.E. Kokorina [d], I.A. Nekrasov [d], V.A. Gavrichkov [a], C. Draxl [e], S.G. Ovchinnikov [a]

[a] Kirensky Institute of Physics SB RAS, Krasnoyarsk 660036, Russia
[b] Reshetnev Siberian State Aerospace University, Krasnoyarsk 660014, Russia
[c] Materials Center Leoben Forschung GmbH, Rosegger-Straße 18, A-8700 Leoben, Austria
[d] Institute of Electrophysics UB RAS, Amundsena Str. 106, 620016 Yekaterinburg, Russia
[e] Physics Department and IRIS Adlershof, Humboldt-Universität zu Berlin, Zum Großen Windkanal 6, 12489 Berlin, Germany

ARTICLE INFO

Article history:
Received 12 December 2014
Received in revised form
13 May 2015
Accepted 18 May 2015
Available online 19 June 2015

Keywords:
High-temperature superconductivity
Electron-phonon coupling
Density-functional theory
Generalized tight-binding approach

ABSTRACT

We present results for the electron-phonon interaction of the Γ-point phonons in the tetragonal high-temperature phase of La_2CuO_4 obtained from a hybrid scheme, combining density-functional theory (DFT) with the generalized tight-binding approach. As a starting point, eigenfrequencies and eigenvectors for the Γ-point phonons are determined from DFT within the frozen phonon approach utilizing the augmented plane wave + local orbitals method. The so obtained characteristics of electron-phonon coupling are converted into parameters of the generalized tight-binding method. This approach is a version of cluster perturbation theory and takes the strong on-site electron correlations into account. The obtained parameters describe the interaction of phonons with Hubbard fermions which form quasiparticle bands in strongly correlated electron systems. As a result, it is found that the Γ-point phonons with the strongest electron-phonon interaction are the A_{2u} modes (236 cm^{-1}, 131 cm^{-1} and 476 cm^{-1}). Finally it is shown, that the single-electron spectral-weight redistribution between different Hubbard fermion quasiparticles results in a suppression of electron-phonon interaction which is strongest for the triplet Hubbard band with *z* oriented copper and oxygen electrons.

1. Introduction

Many physical properties of solids are affected by electron-phonon coupling (EPC), with its most striking manifestation being superconductivity in metals. While in high-T_c compounds the effect of EPC is also well documented [1–3] its crucial role is under debate. The interpretation of the superconducting mechanism in these materials is complicated since intrinsic strong electron correlations can both induce interactions that compete with EPC in the pairing and/or modify electron-phonon coupling along with properties caused by it. To disentangle the impact of electron-electron and electron-phonon interaction in correlated materials, new experimental and theoretical tools are needed.

Recently an experimental attempt in this direction has been carried out using femtosecond spectroscopy on $Bi_2Sr_2Ca_{0.92}Y_{0.08}Cu_2O_{8+\delta}$ crystals with simultaneous time and frequency resolution [4]. Analyzing the different temporal evolutions of electronic and phononic contributions to the total pairing interaction function the authors have revealed a dominant role of the electronic mechanisms of pairing (~80%) with a minor contribution (~20%) of EPC. This very interesting approach requires deeper theoretical analysis. In Eliashberg theory [5] the total interaction determines both, the pairing and the renormalization of electron dispersion in the normal phase. A mean-field analysis [6] of gap equation and isotope effect, simultaneously accounting for strong electron correlation and EPC, exhibited a similar role of magnetic and electron-phonon coupling in the paring mechanism of high-T_c cuprates. On the other hand, an analogous approach to the Migdal-Eliashberg theory developed for the extended Hubbard model, with the self-energy

* Corresponding author. Kirensky Institute of Physics SB RAS, Akademgorodok 50, Bld. 38, Krasnoyarsk 660036, Russia.
E-mail address: shneyder@iph.krasn.ru (E.I. Shneyder).

http://dx.doi.org/10.1016/j.jallcom.2015.05.150
0925-8388/

defined in a non-crossing approach, revealed only small contributions of phonons to the superconducting pairing compared to spin fluctuations induced by strong kinematic interaction [7]. Thus the problem of disentangling the electronic and phononic degrees of freedom is far from being settled.

A theoretical study of the systems in which both, the electron-electron and the electron-phonon interaction, are treated on equal footing, requires band structure, electron self-energy, and polarization operators to be obtained self-consistently. It is obvious that the competition of these interactions can result in different physics [7–9] depending on both the considered model and the relevant physical parameters. Therefore, realistic approaches are required. Since density-functional theory (DFT) within the local-density approximation (LDA) or the generalized gradient approximation (GGA) fails to describe strongly correlated systems, other approaches have been proposed [10,11]. Combining DFT with dynamical mean field theory (DMFT) [12] and/or the *GW* approach, these methods are often computationally highly demanding, but still not necessarily parameter-free. For explaining properties of metals caused by EPC in the normal and the superconducting state, the advantages of DFT and model considerations have been successfully combined [13] by utilizing *ab initio* calculated [14–16] EPC matrix elements and spectral functions that characterize electron-phonon scattering within many-body theory [17–20].

In this paper, we suggest such a *hybrid scheme* for materials with strong electron correlations. To this extent, we convert the characteristics of EPC as obtained in the single-electron LDA picture into parameters of the generalized tight-binding method (GTB) [21]. We then describe the interaction of phonons with Hubbard fermions which form quasiparticle bands. The GTB approach has been proposed earlier to study the electronic structure of strongly correlated electron systems as a generalization of Hubbard's ideas for realistic multi-band models. This method combines the exact diagonalization of the intracell part of the Hamiltonian with the construction of Hubbard operators on the basis of the exact intracell multi-electron eigenstates, and the perturbational treatment of the inter-cell hoppings and interactions. A similar approach for the 3-band $p-d$ model [22,23] of cuprates is known as the cell perturbation theory [24–27].

We apply the GTB approach to the problem of EPC in the strongly correlated electron system La_2CuO_4. In a first step, we perform a transformation [28] of the single-electron LDA wave functions into localized Wannier states with the symmetry corresponding to a realistic multi-band $p-d$ model. In a second step, we obtain multi-electron wave functions of the unit cell by exact diagonalization of the intracell part of the multi-band $p-d$ model Hamiltonian with parameters [29] calculated *ab initio* within the Wannier basis. In a third step, we construct the Hubbard operators to describe electrons as a linear combination of quasi-particles that are excitations containing different local multi-electron states with n and $(n+1)$ electrons. Finally, we derive a relation between EPC matrix elements of conventional band theory and their counterparts for Hubbard fermions.

The paper is organized in the following way: The combined method for studying the coupling of Hubbard fermions with phonons in correlated systems is described in Section 2. Section 3 provides the computational details for the augmented plane wave + local orbitals method, used for obtaining the phonon eigenvectors and eigenfrequencies for La_2CuO_4 that are presented in Section 4. EPC matrix elements are presented in Section 5. Section 6 is dedicated to the discussion of our results.

2. Theoretical background

To properly evaluate the EPC matrix elements in a correlated material we should take into consideration that we cannot rely on the Kohn-Sham band structure based on semi-local exchange-correlation functionals being a good approximation to the quasi-particle bands. Indeed, the band structure of strongly correlated electrons in cuprates looks like the quasi-particle band-structure of Hubbard fermions resulting from a multi-electron approach like LDA + DMFT [30–33] or LDA + GTB [34]. While LDA results in an incorrect metallic state of La_2CuO_4, the GTB method reproduces the charge-transfer insulator for the undoped system and a strong redistribution of spectral weight between Hubbard subbands upon hole doping in underdoped $La_{2-x}Sr_xCuO_4$ [28].

From the very beginning the GTB method, accounting for strong electron correlations, has been suggested for the description of Mott-Hubbard insulators like transition metal oxides. As any other cluster perturbation theory, the GTB method starts with the exact diagonalization of the intracell part of the multi-electron Hamiltonian and treats the intercell part within perturbation theory. The exact diagonalization of the intracell Hamiltonian results in a complete set of orthogonal and normalized eigenstates $\{|p\rangle\}$ and allows for constructing the Hubbard operators $X_f^{p,p'} = |p\rangle\langle p'|$. With this definition any local operator can be represented as a linear combination of X-operators. For example the electron (hole) destruction operator in the cell f with the band index λ takes the form

$$a_{f,\lambda,\sigma} = \sum_{p,p'} |p\rangle\langle p|a_{f,\lambda,\sigma}|p'\rangle\langle p'| = \sum_{p,p'} \gamma_{\lambda,\sigma}(p,p')X_f^{pp'}. \quad (1)$$

Eq. (1) clearly shows the difference in the Fermi type quasi-particle description in the single electron language and in the multielectron one. The operator $a_{f,\lambda,\sigma}$ decreases the number of electrons (holes) by one for all sectors of the Hilbert space simultaneously, while the $X_f^{p,p'}$ operators describe the partial process of electron (hole) removal in the $(N+1)$-electron (hole) configuration $|p'\rangle$, with the final N-electron (hole) configuration $|p\rangle$. The matrix element $\gamma_{\lambda,\sigma} = \langle p|a_{f,\lambda,\sigma}|p'\rangle$ gives the probability of such a process. The splitting of an electron (hole) into different Hubbard fermions stated by Eq. (1) and the following spectral weight redistribution over these quasiparticles are the underlying effects of band structure formation in correlated systems.

In conventional metals, the Hamiltonian describing electron-phonon interaction takes the form

$$H_{\mathrm{EPC}} = \sum_{\mathbf{k},\mathbf{q},\nu,\lambda,\sigma} g_\lambda(\mathbf{k},\mathbf{q};\nu)a^\dagger_{\mathbf{k}+\mathbf{q},\lambda,\sigma}a_{\mathbf{k},\lambda,\sigma}\varphi^\nu_{\mathbf{q}}. \quad (2)$$

Here $\varphi^\nu_{\mathbf{q}}$ is defined as $b_{\mathbf{q},\nu} + b^\dagger_{-\mathbf{q},\nu}$, where $b_{\mathbf{q},\nu}(b^\dagger_{-\mathbf{q},\nu})$ is the annihilation (creation) operator of a phonon of branch ν and momentum $\mathbf{q}$. The operators $a_{\mathbf{k},\lambda,\sigma}$ and $a^\dagger_{\mathbf{k},\lambda,\sigma}$ describe the annihilation and creation, respectively, of an electron with spin σ and initial momentum $\mathbf{k}$ in band λ. Parameter $g_\lambda(\mathbf{k},\mathbf{q};\nu)$ is the corresponding EPC matrix element. To take effects of strong electron correlations into account and describe the interaction of phonons with Hubbard fermions forming a quasiparticle band structure we will rewrite the Hamiltonian (2) in the representation (1) of the Hubbard operators following the procedure of the GTB method.

For this purpose we proceed with a realistic microscopical model of the La_2CuO_4 system which reflects its chemical structure and contains a proper description of its low-energy physics [35]. In the hole representation that is more convenient for cuprates the

initial multiband Hamiltonian is given by

$$H_{pd} = \sum_{f,\lambda,\sigma} (\varepsilon_\lambda - \mu) n_{f,\lambda,\sigma} + \sum_{f \neq g} \sum_{\lambda,\lambda',\sigma} T_{fg}^{\lambda\lambda'} c_{f,\lambda,\sigma}^{\dagger} c_{g,\lambda',\sigma} + \\ + \frac{1}{2} \sum_{f,g,\lambda,\lambda'} \sum_{\sigma_{1,2,3,4}} V_{fg}^{\lambda\lambda'} c_{f,\lambda,\sigma_1}^{\dagger} c_{f,\lambda,\sigma_3} c_{g,\lambda',\sigma_2}^{\dagger} c_{g,\lambda',\sigma_4}. \quad (3)$$

Here $c_{f,\lambda,\sigma}$ is the annihilation operator in Wannier representation of the hole at orbital λ with spin σ, and $n_{f,\lambda,\sigma} = c_{f,\lambda,\sigma}^{\dagger} c_{f,\lambda,\sigma}$. Index λ indicates the copper orbitals $d_{x^2-y^2}$ and $d_{3z^2-r^2}$, the plane-oxygen orbitals p_x and p_y, and the p_z orbitals of the apical oxygen. Thereby index f runs through the positions of copper and oxygen atomic orbitals and ε_λ denotes the single-electron energy of the corresponding atomic orbital λ. Parameter $T_{fg}^{\lambda\lambda'}$ includes the hopping matrix elements between copper and oxygen orbitals and between oxygen and oxygen ones. These are the parameter t_{pd} for the hopping between $d_{x^2-y^2}$ and p_x, p_y orbitals, $t_{pd}/\sqrt{3}$ for the $d_{3z^2-r^2} \leftrightarrow p_x, p_y$ hopping, t'_{pd} for the $d_{3z^2-r^2} \leftrightarrow p_z$ hopping, t_{pp} for hopping $p_x \leftrightarrow p_y$, and t'_{pp} for hopping between p_x, p_y and p_z orbitals. The Coulomb matrix elements $V_{fg}^{\lambda\lambda'}$ include intraorbital Hubbard repulsion energies U_d and U_p of two holes with opposite spins on copper $d_{x^2-y^2}$, $d_{3z^2-r^2}$ and oxygen p_x, p_y, and p_z orbitals respectively, interorbital Coulomb repulsion energy V_d and V_p, Hund's exchange interaction on copper J_d and oxygen J_p orbitals, and the nearest-neighbor copper-oxygen Coulomb repulsion V_{pd}.

The *ab initio* hopping parameters and single electron energies of the multiband $p-d$ model (3) for La_2CuO_4 have been obtained [29] earlier using a Wannier function projection procedure [36]. Their values are listed in Table 1 and differ from the values in the Table III of Ref [29] since we do not normalize them by t_{pd}. Values of Coulomb parameters have been obtained [37,38] by fitting to experimental ARPES data which resulted in the following parameters: $U_d = V_d = 9$, $U_p = V_p = 4$, $J_d = 1$, $J_p = 0$, $V_{pd} = 1.5$ (all values are given in eV).

The exact diagonalization of the unit cell Hamiltonian (3) was performed in a work [35], where the problem of non-orthogonality of the molecular orbitals of neighboring CuO_6 clusters was solved explicitly via diagonalization in k-space [40]. In a new symmetric basis the intracell part of the total Hamiltonian is diagonalized, allowing to classify all possible effective quasiparticle excitations according to a symmetry. The new operators of cell orbitals $c_{\mathbf{k},\mu,\sigma}^{cell}$ that diagonalize the unit-cell Hamiltonian are linear combination of initial molecular orbitals, see details elsewhere [35]. Their relationship with the Fourier transformed original hole operators can be presented in the form

$$c_{\mathbf{k},\lambda,\sigma} = \sum_{\mu} \alpha_{\lambda,\mu} c_{\mathbf{k},\mu,\sigma}^{cell}, \quad (4)$$

where index μ runs through the new orbitals of b_1 and a_1 symmetry on the plane-oxygen sites, p_z binding and antibinding orbitals on the apical oxygen, and unmodified $d_{x^2-y^2}$ and $d_{3z^2-r^2}$ orbitals on copper.

To get the matrix elements $\gamma_{\lambda,\sigma} = \langle p | a_{f,\lambda,\sigma} | p' \rangle$ that determine the partial weight of a quasiparticle excitation with spin σ and orbital index λ between intracell states p and p' we repeat the procedure of exact diagonalization of the intracell part of the Hamiltonian (3) with *ab initio* parameters [29,39] for the La_2CuO_4 system. To simplify the problem, we assume that electron-phonon coupling (2) does not change the set of eigenstates $|p\rangle$ and their energies E_p significantly. Since the total number of the cell eigenstates resulting from the diagonalization is more than 100, we proceed with a limited set of eigenstates, which is reasonable as we are interested in the low-energy region. The relevant states are shown in Fig. 1. In the one-hole sector of the Hilbert space formed by d^9p^6 or $d^{10}p^5$ orbital configurations, the lowest eigenstate is the spin doublet $|\sigma\rangle \equiv \{|\uparrow\rangle, |\downarrow\rangle\}$ with b_{1g} orbital symmetry. The lowest two-hole states formed by d^9p^5, $d^{10}p^4$ or d^8p^6 orbital configurations are the Zhang-Rice singlet $|S\rangle$ with ${}^1A_{1g}$ symmetry and ${}^3B_{1g}$ triplet states $|T_M\rangle \equiv \{|T_{M=0}\rangle, |T_{M=2\sigma}\rangle, |T_{M=-2\sigma}\rangle\}$. Therefore the matrix elements $\langle p | c_{f,\mu,\sigma}^{cell} | p' \rangle$ are defined in the minimal realistic basis $|p\rangle = \{|\sigma\rangle, |S\rangle, |T_M\rangle\}$ which corresponds to an effective low-energy singlet-triplet model.

Now we can rewrite the Hamiltonian (2) in the representation of the Hubbard operators. Based on definitions (1) and (4) the expression for electron-phonon interaction (2) in systems with strong electron correlation (SEC) takes the form

$$H_{\mathrm{EPC}} = \sum_{\mathbf{k},\mathbf{q},\sigma,\nu} \sum_{m,n} g_{mn}^{SEC}(\mathbf{k},\mathbf{q};\nu) X_{\mathbf{k}+\mathbf{q}}^{\dagger m} X_{\mathbf{k}}^{n} \varphi_{\mathbf{q}}^{\nu} \quad (5)$$

with the matrix element for Hubbard fermion-phonon coupling g_{mn}^{SEC} defined as

$$g_{mn}^{SEC} = \sum_{\lambda,\mu,\mu'} g_{\lambda}(\mathbf{k},\mathbf{q};\nu) \alpha_{\lambda\mu}^{*} \alpha_{\lambda\mu'} \gamma_{\mu\sigma}^{*}(m) \gamma_{\mu'\sigma}(n). \quad (6)$$

Here, index $m \leftrightarrow (p,p')$ enumerates the quasiparticle excitations between intracell states p and p' with energy $\omega_m = \varepsilon_p(N+1) - \varepsilon_{p'}(N)$, where ε_p is the p-th energy level of the N-electron system. Corresponding quasiparticle bands m are formed by these excitations due to perturbation treatment of the intercell hopping and interactions at the next step of GTB approach [35]. It should be stressed that the GTB bands do not correspond to the

Table 1
Hopping parameters and single-electron energies of the multiband $p-d$ model (3) obtained in the framework of the LDA + GTB method [29] and used in the present paper. In contrast to the values reported in Ref. [29], the values here are not normalized by t_{pd}.

Parameter	$\varepsilon_{d_{x^2-y^2}}$	$\varepsilon_{d_{3z^2-r^2}}$	ε_{p_x,p_y}	ε_{p_z}	t_{pd}	t'_{pd}	t_{pp}	t'_{pp}
Value, eV	0	0.14	0.91	−0.26	1.36	0.77	0.86	0.39

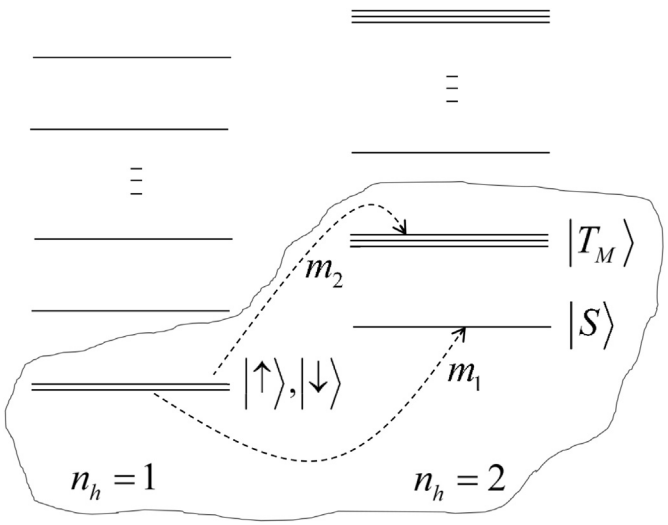

Fig. 1. Schematic picture of the local states obtained by exact diagonalization of the multiband Hamiltonian (3) for the CuO_6 cluster. The procedure of diagonalization is performed separately for each sector of the Hilbert space with the given number of holes per unit cell $n_h = 1, 2$. Dashed lines with arrows show quasiparticle excitations between different local states.

conventional definition of a band structure. Instead, these bands are formed by quasiparticle excitations between different multi-electron configurations, and the number of states in each particular band depends on the occupation number of the initial and final multi-electron configurations, and thus on the electron occupation.

3. Computational details

In order to obtain optimized lattice constants and atomic positions as a starting point for frozen-phonon calculations, the augmented plane wave + local orbital (APW + lo) method [41] implemented in the WIEN2k code [42] is used. This method provides the most accurate way to treat crystals within density-functional theory. At this stage, exchange and correlation effects are treated within the local density approximation (LDA). The atomic sphere radii R_{MT} were chosen as 2.4 a.u. for La, 1.875 a.u. for Cu, and 1.575 a.u. for the O atoms. For the wavefunctions, a plane wave cutoff $K_{max} = 4.44$ was used, which corresponds to about 970 basis functions and $R_{MT} \times K_{max}$ values of 10.67 for La, 8.33 for Cu, and 7.0 for O, respectively. We used 512 **k** points in the full Brillouin zone (BZ) for the self-consistency cycles, which yields 56 points in the irreducible wedge. The plane wave cutoff for expanding charge density and potential in the interstitial region, G_{max}, was 14.

All degrees of freedom, *i.e.*, the atomic positions and the lattice constants, were optimized starting from the experimental ones as reported in Ref. [43]. The space group of La_2CuO_4 in the tetragonal phase is *I*4/*mmm* (no. 139).

The structure with the lowest total energy is found for a = 3.72 Å, c = 12.98 Å, *i.e.*, the volume is about 5% smaller than in experiment. The positions of La and apex oxygen O2 are obtained as (0, 0, 0.3616 c) and (0, 0, 0.184 c), respectively, which implies that the *z* coordinate of the apex oxygen changes by 0.03 Å, while the position of La is not affected by the optimization.

The phonon modes have been obtained in the frozen phonon approximation based on the linearized augmented plane wave (LAPW) method [44–46]. Details about the procedure are found, for example, in Ref. [47]. For each degree of freedom 4 displacements, two in positive and two in negative direction, have been calculated. A linear fit of the resulting forces as a function of displacement has been used to set up the dynamical matrix, which yields the phonon eigenfrequencies and eigenvectors.

4. Γ point phonons from DFT

Table 2 shows the eigenfrequencies and eigenvectors for all Γ point phonons of La_2CuO_4, while Table 3 compares the eigenfrequencies with previous *ab initio* calculations [48–50] and results from infrared (IR) measurements [53,54], neutron diffraction [51], and Raman scattering experiments [52].

In all three theoretical works [48–50] the LAPW method together with the LDA for the exchange-correlation potential was used for the groundstate computations. Compared to these calculations we have used a considerably larger set of basis functions (about 950 compared to 750 in Refs. [48,49] and 650 in Ref. [50]), and the generally more accurate APW + lo scheme. Regarding the lattice constants, Refs. [48] and [49] have used the experimental ones, while Ref. [50] has optimized both the volume and the c/a ratio yielding the same geometry as ours. For the phonon calculations, Refs. [49] and Refs. [50] applied the frozen phonon method, while the results in Ref. [48] are based on linear-response calculations.

Our frequencies for the A_{1g} phonons are—as the ones presented by Cohen et al. [50]—in excellent agreement with experiment. A comparison of these results with the ones obtained without geometry optimization [48,49] demonstrates that the optimized geometry improves the frequencies considerably [55]. A similar situation is found for the A_{2u} modes, where the agreement with experiment is again significantly improved. For the B_{2u} mode the situation is similar: our frequency of 227 cm^{-1} is about 10% higher than the one obtained with experimental geometry [48,49] and thus closer to the result of 270 cm^{-1} obtained by neutron diffraction [51]. Surprisingly, Cohen et al. [50] report 293 cm^{-1} for the same mode, even though the latter used a very similar method and the same geometry as it has been used in our calculations. Analyzing, finally, the results for the E_g and E_u modes, it turns out that our calculations have especially improved the results for the low-frequency modes of either species, where former calculations yielded either extremely low or even imaginary frequencies. This indicates that for the low-energy features the higher accuracy resulting from the larger basis set is especially important.

The eigenvectors are similar to the ones presented in Ref. [48]. A major difference is found for the A_{2u} mode with 236 cm^{-1}, where the eigenvector reported in Ref. [48] has a smaller contribution of La, but a much larger displacement of the Cu atom. The frequency presented in this reference is only 182 cm^{-1}, which indicates that the larger mass of La compared to Cu, which should lead to a lower frequency, is more than compensated by the effect of geometry optimization, where latter yields a result much closer to experiment.

5. Electron-phonon coupling parameters

To extract EPC parameters entering in Eq. (2), we have computed the electronic band structure for the equilibrium structure as well as the band structure with ionic displacements for each Γ point phonon mode. For each case, the difference between the Kohn-

Table 2
Calculated eigenfrequencies (in cm^{-1}) and eigenvectors of the Γ point modes of La_2CuO_4. The eigenvectors in each row are normalized to unity. The detailed definition of the eigenvectors is given in Eq. (7).

Mode	ω (cm^{-1})	La_x	La_y	La_z	$Cu_{x,y}$	Cu_z	$O1_x$	$O1_y$	$O1_z$	$O2_x$	$O2_y$	$O2_z$
A_{1g}	415	–	–	0.076	–	–	–	–	–	–	–	0.997
	232	–	–	0.997	–	–	–	–	–	–	–	−0.076
A_{2u}	476	–	–	−0.10	–	0.04	–	–	−0.57	–	–	0.81
	236	–	–	0.38	–	0.07	–	–	−0.77	–	–	−0.50
	131	–	–	0.44	–	−0.90	–	–	0.02	–	–	0.14
B_{2u}	227	–	–	–	–	–	–	–	1.00	–	–	–
E_g	209	−0.20	0.20	–	–	–	–	–	–	0.68	−0.68	–
	73	0.68	−0.68	–	–	–	–	–	–	0.20	−0.20	–
E_u	727	0.00	0.00	–	0.26	–	0.09	−0.96	–	0.024	0.02	–
	341	0.05	0.05	–	0.28	–	−0.95	0.05	–	−0.05	−0.05	–
	210	0.19	0.19	–	−0.83	–	−0.34	−0.34	–	0.05	0.05	–
	80	0.14	0.14	–	−0.02	–	0.07	−0.04	–	−0.69	−0.69	–

Table 3
Calculated eigenfrequencies (in cm^{-1}) of the Γ point phonons compared to literature. Papers [48–50] refer to DFT calculations using LDA, papers [53] and [54] to infrared measurements, and paper [52] to a Raman scattering experiment. The frequencies reported for neutron diffraction are extracted [51] from data of $La_{1.9}Sr_{0.1}CuO_4$ at 295 K.

	This	Literature					
	Work	LDA [48]	LDA [49]	LDA [50]	IR	Neutron [51]	Raman [52]
A_{1g}	415	375	390	415	–	427	433
	232	202	215	224	–	227	226
A_{2u}	476	441	446	–	500 [53], 501 [54]	497	–
	236	182	197	–	235 [53], 342 [54]	251	–
	131	132	119	–	135 [53], 242 [54]	149	–
B_{2u}	227	193	201	293	–	270	–
E_g	209	201	212	233	–	241	–
	73	26	15		–	91	–
E_u	727	630	650	–	695 [54]	684	–
	341	319	312	–	360 [54]	354	–
	209	147	146	–	140 [54]	173	–
	80	22	75i	39		126	–

Sham eigenvalues of the distorted and undistorted system has been extracted. To do so, we have used LDA band structure calculations within the linearized muffin-tin orbitals method [44–46] with default settings. (The version name of the applied code is TB-LMTO v.47). To get the distorted crystal structure in accordance with the phonon eigenvectors of different phonon modes described in the previous sections we introduce ionic displacements which are small enough to stay within linear regime, but still get sizable changes of the band structure.

In order to compare the electron-phonon coupling parameters for the different phonon modes with each other, the displacements are normalized to obtain the dimensionless phonon coordinate Q defined as [56].

$$Q\sqrt{\frac{\hbar}{M_\alpha\omega_\beta}}\mathbf{e}_{\alpha\beta}=\mathbf{u}^\alpha_\beta. \tag{7}$$

Here, ω_β is the eigenfrequency of the considered mode, M_α is the mass of ion α and $\mathbf{u}^\alpha_\beta$ is the corresponding real displacement.

The results for $\mathbf{k}=0$ are given in Table 4. In order to investigate the dependence of the electronic structure on phonon displacements, we consider the 6 bands with predominant contribution of Cu-$d_{x^2-y^2}$ and Cu-$d_{3z^2-r^2}$ orbitals, p_x and p_y orbitals of the in-plane oxygen O1, and p_z orbitals of the apex oxygen O2. Such a set of bands corresponds to a 5-band $p-d$ model and provides a proper description of LDA bands near the Fermi level. The electron-phonon interaction is very different for the different phonon modes: it is small for all bands for both E_g modes as well as the E_u modes with 209 cm^{-1} and 80 cm^{-1}, and already an order of magnitude larger for the O1-p_x, p_y bands in case of the E_u modes with 727 and 341 cm^{-1}. All of the A_{1g} modes exhibit considerable coupling to the O2-p_z bands and O1-p_x, p_y bands. The same four bands and also the Cu-$d_{3z^2-r^2}$ band are the most affected ones in case of the B_{2u} phonon mode. The strongest EPC, however, is exhibited by the three A_{2u} modes, which especially alter the O1-p_x, p_y, O2-p_z, and Cu-$d_{3z^2-r^2}$ levels.

Table 4
Absolute value (in eV) of electron-phonon interaction parameters at the Γ point for the different bands and phonon modes. The numbers in the first column correspond to the frequencies of the mode.

	ω (cm^{-1})	Band, λ					
		Cu-$d_{x^2-y^2}$	Cu-$d_{3z^2-r^2}$	O1-2p_x	O1-2p_y	O2-p_z(1)	O2-p_z(2)
A_{1g}	415	0.137	0.137	0.776	0.776	2.147	1.462
	232	0.264	0.616	0.459	0.459	1.398	0.713
A_{2u}	476	0.517	0.765	1.335	1.335	2.755	1.042
	236	2.701	3.913	8.806	8.806	3.791	1.054
	131	0.829	1.557	3.132	3.132	3.332	0.692
B_{2u}	227	0.082	0.519	0.585	0.585	1.029	0.239
E_g	209	0.036	0.125	0.073	0.073	0.048	0.273
	73	0.015	0.059	0.278	0.254	0.039	0.161
E_u	727	0.320	0.232	1.038	1.093	0.784	0.342
	341	0.198	0.568	1.366	1.568	1.213	0.568
	209	0.053	0.059	0.133	0.149	0.156	0.108
	80	0.060	0.213	0.132	0.118	0.155	0.198

6. Renormalization of EPC constants by electron correlation

The parameters $g^{SEC}_{mn}(\mathbf{k},\mathbf{q};\nu)$ of interaction between Hubbard fermions and Γ-point phonons at $\mathbf{k}=\mathbf{0}$ are calculated via the Eq. (6) with coefficients $\alpha_{\lambda\mu}$ and $\gamma_{\mu\sigma}$ described in Section 2. Results are presented in Table 5 for singlet and triplet bands. The quasiparticle excitations $m_1=(\pm\sigma, S)$ and $m_2=\{(\pm\sigma, T_{\pm M}),(\pm\sigma, T_{M=0})\}$ which form these bands are schematically shown in Fig. 1. Since the number of states in each particular band depends on the occupation number of the initial and final multielectron configurations, Eqs. (5) and (6) are valid when the singlet band becomes conducting due to doping.

Analysis of the data in Table 5 shows that for each given quasiparticle band m the strongest interactions are exhibited by A_{2u} modes with 236 and 131 cm^{-1}, while E_g modes and E_u ones with 209 and 80 cm^{-1} demonstrate the smallest coupling. It completely agrees with the features of electron-phonon interaction determined for a given band λ in Table 4. The origin of the strong coupling in the A_{2u} modes is a poor screening of the Coulomb potential perpendicular to the conducting CuO_2 layers [57,2] that results in a strong modulation of the Madelung potential by c-axes phonons. A direct proof of strong coupling between electrons and

Table 5
Absolute value of Hubbard fermion-phonon interaction (in eV).

Mode	ω (cm^{-1})	Quasiparticle band, m		
		(σ, S)	$(\pm\sigma, T_{\pm 2\sigma})$	$(\pm\sigma, T_{M=0})$
A_{1g}	415	0.688	1.492	0.746
	232	0.552	0.969	0.485
A_{2u}	476	1.065	1.695	0.848
	236	7.325	1.683	0.841
	131	2.661	1.899	0.950
B_{2u}	227	0.035	0.403	0.201
E_g	209	0.085	0.111	0.056
	73	0.249	0.076	0.038
E_u	727	1.158	0.503	0.252
	341	1.492	0.824	0.412
	209	0.158	0.118	0.059
	80	0.145	0.177	0.089

ionic displacements along the *c*-axes was the colossal heat expansion of La_2 CuO_4 under high-power femtosecond light irradiation [58]. In this experiment a sudden increase of the *c*-lattice parameter induced by photodoped holes has been observed.

A comparison of the maximum values of interaction in Tables 4 and 5 for each given mode shows their reduction in the limit of strong electron correlation (Table 5) by approximately 20–30 percent, with insignificant exceptions for two E_u modes. This effect is caused by redistribution of single electron spectral weight between Hubbard subbands as follows from Eqs. (1), (5) and (6). Consider, e.g., the A_{2u} mode with 131 cm^{-1}. In this case the maximal value of the Hubbard fermion-phonon coupling is observed for the singlet band m_1 (Fig. 1), and $g^{SEC}_{m_1,m_1}(\mathbf{k}=0,\mathbf{q}=0)\approx 2.7$ eV. The quasiparticle excitation m_1 from the doublet state $|\sigma\rangle$ to the singlet one $|S\rangle$ correspond to the creation (destruction) of a hole in the state formed by approximately 80% of b_1 plane oxygen orbital and 20% of copper $d_{x^2-y^2}$ orbitals. Making use of the data from Table 4 we can estimate the value of the Hubbard fermion coupling $g^{SEC}_{m_1,m_1}$: $0.8g_{\lambda=p_{x,y}}+0.2g_{\lambda=d_{x^2-y^2}}\approx 2.7$.

7. Discussions

In summary, we have applied a method combining density-functional theory and the generalized tight-binding approach for studying electron-phonon coupling in the strongly correlated system. We demonstrate that strong electron correlation leads to suppression of electron-phonon coupling, or, more precisely, of the interaction parameters between Hubbard fermions and phonons, due to spectral weight redistribution over Hubbard fermions. Earlier effects of electron-phonon interaction in strongly correlated materials have been studied in the two-dimensional Hubbard model by employing dynamical cluster Monte Carlo calculations [59]. It was obtained that strong suppression of the single-particle quasiparticle weight leads to strong renormalization of the single-particle propagator and therefore results in suppression of the superconductivity. Moderate suppression of electron-phonon coupling by Coulomb interaction had been obtained also in the Holstein-Hubbard model using the dynamical mean-field approximation [60].

The presented analysis revealing modification of electron-phonon interaction in systems with strong electron correlation is far from being completed. Nevertheless we believe that the main peculiarities of the interaction between phonons and strongly correlated electrons are elucidated here. Generally there are two obvious possibilities to analyze the strong electron-phonon interaction in systems with strong electron correlations. In one case, the interaction of electrons with the lattice vibrations altering the spectrum of electrons results in polaron effects. In many other cases, the electron-phonon interaction can be treated perturbatively since phonons interact with formed quasiparticles. The method proposed above differs from a conventional band approach in the definition of these quasiparticles. Indeed Hubbard quasiparticles are forming under conditions of weakly screened Coulomb interaction, when double occupied states are shifted to high energies by the large on-site electron-electron coupling. The main effect of this redefinition of quasiparticles is the redistribution of the spectral weight between Hubbard excitations that results in the reduction of the coupling constant between electron excitations and phonons.

Acknowledgment

We acknowledge the stimulating discussions with V.V. Val'kov, D.M. Dzebisashvilly, M.M. Korshunov and I.S. Sandalov. E.I.S. and S.G.O. are thankful to the Russian Science Foundation (project No. 14-12-00061) for the support of the research given in Sections 2, 6 and 7. E.E.K. and I.A.N. are thankful to the State Contract No. 0389-2014-0001 and RFBR grant No. 14-02-00065 for the support of the research given in Section 5. Financial support of the research given in Sections 3 and 4 by the Austrian Federal Government (in particular from Bundesministerium für Verkehr, Innovation und Technologie and Bundesministerium für Wissenschaft, Forschung und Wirtschaft) represented by Österreichische Forschungsförderungsgesellschaft mbH and the Styrian and the Tyrolean Provincial Government, represented by Steirische Wirtschaftsförderungsgesellschaft mbH and Standortagentur Tirol, within the framework of the COMET Funding Programme is gratefully acknowledged by C.D. and J.S.

References

[1] E.G. Maksimov, M.L. Kulić, O.V. Dolgov, Bosonic spectral function and the electron–phonon interaction in htsc cuprates, Adv. Cond. Matter Phys. 2010 (2010) 1–64, http://dx.doi.org/10.1155/2010/423725.
[2] M. Kulić, O.V. Dolgov, Forward scattering peak in the electron-phonon interaction and impurity scattering of cuprate superconductors, Phys. Stat. Sol. B 242 (2005) 151–178, http://dx.doi.org/10.1002/pssb.200404956.
[3] E.G. Maksimov, High-temperature superconductivity: the current state, Phys. Usp. 43 (2000) 965–990, http://dx.doi.org/10.1070/PU2000v043n10ABEH000770.
[4] S.D. Conte, C. Giannetti, G. Coslovich, F. Cilento, D. Bossini, T. Abebaw, F. Banfi, G. Ferrini, H. Eisaki, M. Greven, A. Damascelli, D. van der Marel, F. Parmigiani, Disentangling the electronic and phononic glue in a high-Tc superconductor, Science 335 (2012) 1600–1603, http://dx.doi.org/10.1126/science.1216765.
[5] G.M. Eliashberg, Electron-phonon interactions and superconductivity, Sov. Phys. JETP 11 (1960) 696–702.
[6] S.G. Ovchinnikov, E.I. Shneyder, The interplay of phonon and magnetic mechanism of pairing in strongly correlated electron system of high-Tc cuprates, J. Supercond. Nov. Magn. 23 (2010) 733–736, http://dx.doi.org/10.1007/s10948-009-0633-z.
[7] N.M. Plakida, V.S. Oudovenko, On the theory of superconductivity in the extended hubbard model, Eur. Phys. J. B 86 (2013) 115, http://dx.doi.org/10.1140/epjb/e2013-31157-6.
[8] M. Sadovskii, E. Kuchinskii, I. Nekrasov, Interplay of electron-phonon interaction and strong correlations: DMFT+ σ approach, J. Phys. Chem. Solids 72 (2011) 366–370, http://dx.doi.org/10.1016/j.jpcs.2010.10.082.
[9] M. Capone, C. Castellani, M. Grilli, Electron–phonon interaction in strongly correlated systems, Adv. Cond. Matter Phys. 2010 (2010) 18, http://dx.doi.org/10.1155/2010/920860.
[10] S. Savrasov, G. Kotliar, Linear response calculations of lattice dynamics in strongly correlated systems, Phys. Rev. Lett. 90 (2003), 056401–. http://dx.doi.org/10.1103/PhysRevLett.90.056401.
[11] Z. Yin, A. Kutepov, G. Kotliar, Correlation-enhanced electron-phonon coupling: applications of gw and screened hybrid functional to bismuthates, chloronitrides, and other high Tc superconductors, Phys. Rev. X 3 (2013) 021011, http://dx.doi.org/10.1103/PhysRevX.3.021011.
[12] A. Georges, G. Kotliar, W. Krauth, M. Rozenberg, Dynamical mean-field theory of strongly correlated fermion systems and the limit of infinite dimensions, Rev. Mod. Phys. 68 (1996) 13. http://dx.doi.org/10.1103/RevModPhys.68.13.
[13] E.G. Maksimov, D. Yu Savrasov, S. Yu Savrasov, The electron–phonon interaction and the physical properties of metals, Phys. Usp. 40 (1997) 337–358, http://dx.doi.org/10.1070/PU1997v040n04ABEH000226.
[14] S. Savrasov, D. Savrasov, O. Andersen, Linear-response calculations of electron–phonon interactions, Phys. Rev. Lett. 72 (1994) 372. http://dx.doi.org/10.1103/PhysRevLett.72.372.
[15] S. Savrasov, Linear-response theory and lattice dynamics: a muffin-tin-orbital approach, Phys. Rev. B 54 (1996) 16470. http://dx.doi.org/10.1103/PhysRevB.54.16470.
[16] S. Savrasov, D. Savrasov, Electron-phonon interactions and related physical properties of metals from linear-response theory, Phys. Rev. B 54 (1996) 16487. http://dx.doi.org/10.1103/PhysRevB.54.16487.
[17] D.J. Scalapino, The electron–phonon interaction and strong-coupling superconductors, in: R.D. Parks (Ed.), Superconductivity: Part 1 (In Two Parts), CRC Press, NY, 1969, pp. 449–560. ISBN 0824715209, 9780824715205.
[18] D. Rainer, Principles of *ab initio* calculations of superconducting transition temperatures, in: D.F. Brewer (Ed.), Progress in Low Temperature Physics, Elsevier, Amsterdam, 1986, pp. 371–424.
[19] P.B. Allen, B. Mitrovic, Theory of superconducting Tc, in: H. Ehrenreich, F. Zeitz, D. Turnbull (Eds.), Solid State Physics, Acad. Press, NY, 1982, pp. 371–424. ISBN: 978-0-12-607736-0.
[20] O.V. Dolgov, E.G. Maksimov, Transition temperature of strong-coupling superconductors, Sov. Phys. Usp. 25 (1982) 688, http://dx.doi.org/10.1070/PU1982v025n09ABEH004602.
[21] S.G. Ovchinnikov, I.S. Sandalov, The band structure of strong-correlated electrons in $La_{2x}Sr_xCuO_4$ and $YBa_2Cu_3O_{7y}$, Phys. C 161 (1989) 607–617,

http://dx.doi.org/10.1016/0921-4534(89)90397-3.
[22] V. Emery, Theory of high-Tc superconductivity in oxides, Phys. Rev. Lett. 58 (1987) 2794. http://dx.doi.org/10.1103/PhysRevLett.58.2794.
[23] C.M. Varma, S. Smitt-Rink, E. Abrahams, Charge transfer excitations and superconductivity in "ionic" metals, Solid State Commun. 62 (1987) 681–685, http://dx.doi.org/10.1016/0038-1098(87)90407-8.
[24] S.V. Lovtsov, V.Y. Yushankhai, Effective singlet-triplet model for CuO_2 plane in oxide superconductors: the change fluctuation regime, Phys. C 179 (1991) 159–166, http://dx.doi.org/10.1016/0921-4534(91)90024-S.
[25] J.H. Jefferson, H. Eskes, L.F. Feiner, Derivation of a single-band model for CuO_2 planes by a cell-perturbation method, Phys. Rev. B 45 (1992) 7959. http://dx.doi.org/10.1103/PhysRevB.45.7959.
[26] H.-B. Schüttler, A. Fedro, Copper-oxygen charge excitations and the effective-single-band theory of cuprate superconductors, Phys. Rev. B 45 (1992), 7588(R), http://dx.doi.org/10.1103/PhysRevB.45.7588.
[27] N.M. Plakida, V.S. Oudovenko, Electron spectrum and superconductivity in the t-j model at moderate doping, Phys. Rev. B 59 (1999) 11949. http://dx.doi.org/10.1103/PhysRevB.59.11949.
[28] V.A. Gavrichkov, A.A. Borisov, S.G. Ovchinnikov, Angle-resolved photoemission data and quasiparticle spectra in antiferromagnetic insulators $Sr_2CuO_2Cl_2$ and $Ca_2CuO_2Cl_2$, Phys. Rev. B 64 (2001) 235124. http://dx.doi.org/10.1103/PhysRevB.64.235124.
[29] M.M. Korshunov, V.A. Gavrichkov, I.A. Nekrasov, Z.V. Pchelkina, V.I. Anisimov, Hybrid LDA and generalized tight-binding method for electronic structure calculations of strongly correlated electron systems, Phys. Rev. B 72 (2005) 165104, http://dx.doi.org/10.1103/PhysRevB.72.165104.
[30] V. Anisimov, A.I. Poteryaev, M.A. Korotin, A.O. Anokhin, G. Kotliar, First-principles calculations of the electronic structure and spectra of strongly correlated systems: dynamical mean-field theory, J. Phys. Condens. Matter 9 (1997) 7359–7368, http://dx.doi.org/10.1088/0953-8984/9/35/010.
[31] A. Lichtenstein, M. Katsnelson, *Ab initio* calculations of quasiparticle band structure in correlated systems: LDA++ approach, Phys. Rev. B 57 (1998) 6884–6895. http://dx.doi.org/10.1103/PhysRevB.57.6884.
[32] K. Held, I.A. Nekrasov, N. Blümer, V.I. Anisimov, D. Vollhardt, Realistic modeling of strongly correlated electron systems: an introduction to the LDA+DMFT approach, Int. J. Mod. Phys. B 15 (2001) 2611–2625, http://dx.doi.org/10.1142/S0217979201006495.
[33] G. Kotliar, S.Y. Savrasov, K. Haule, V.S. Oudovenko, O. Parcollet, C.A. Marianetti, Electronic structure calculations with dynamical mean-field theory, Rev. Mod. Phys. 78 (2006) 865. http://dx.doi.org/10.1103/RevModPhys.78.865.
[34] M.M. Korshunov, S.G. Ovchinnikov, E.I. Shneyder, V.A. Gavrichkov, Y.S. Orlov, I.A. Nekrasov, Z.V. Pchelkina, Cuprates, manganites, and cobaltites: multi-electron approach to the band structure, Mod. Phys. Lett. B 26 (2012) 1230016, http://dx.doi.org/10.1142/S0217984912300165.
[35] V.A. Gavrichkov, S.G. Ovchinnikov, A.A. Borisov, E.G. Goryachev, Evolution of the quasiparticle band structure with doping in copper oxides by the generalized tight-binding method, JETP 91 (2000) 369–383, http://dx.doi.org/10.1134/1.1311997.
[36] A.K.V.I. Anisimov, D.E. Kondakov, I.A. Nekrasov, Z.V. Pchelkina, J.W. Allen, S.-K. Mo, H.-D. Kim, P. Metcalf, S. Suga, A. Sekiyama, G. Keller, I. Leonov, X. Ren, D. Vollhardt, Full orbital calculation scheme for materials with strongly correlated electrons, Phys. Rev. B 71 (2005) 125119. http://dx.doi.org/10.1103/PhysRevB.71.125119.
[37] B. Wells, Z.-X. Shen, A. Matsuura, D. King, M. Kastner, M. Greven, R. Birgeneau, E versus k relations and many body effects in the model insulating copper oxide $Sr_2CuO_2Cl_2$, Phys. Rev. Lett. 74 (1995) 964. http://dx.doi.org/10.1103/PhysRevLett.74.964.
[38] N. Armitage, D. Lu, C. Kim, A. Damascelli, K. Shen, F. Ronning, D. Feng, P. Bogdanov, Z.-X. Shen, Y. Onose, Y. Taguchi, Y. Tokura, P. Mang, N. Kaneko, M. Greven, Anomalous electronic structure and pseudogap effects in $Nd_{1.85}Ce_{0.15}CuO_4$, Phys. Rev. Lett. 87 (2001) 147003. http://dx.doi.org/10.1103/PhysRevLett.87.147003.
[39] V.I. Anisimov, M.A. Korotin, I.A. Nekrasov, Z.V. Pchelkina, S. Sorella, First principles electronic model for high-temperature superconductivity, Phys. Rev. B 66 (2002) 100502. http://dx.doi.org/10.1103/PhysRevB.66.100502.
[40] R. Raimondi, L.F.J.H. Jefferson, Effective single-band models for the high-Tc cuprates. ii. role of apical oxygen, Phys. Rev. B 53 (1996) 8774. http://dx.doi.org/10.1103/PhysRevB.53.8774.
[41] E. Sjöstedt, L. Nordström, D.J. Singh, An alternative way of linearizing the augmented plane-wave method, Solid State Commun. 114 (2000) 15.
[42] P. Blaha, K. Schwarz, J. Luitz, WIEN2k (Release 97.8), [Improved and updated Unix version of the original copyright WIEN code, which was published by P. Blaha, K. Schwarz, P. Sorantin and S. B. Trickey, Comp. Phys. Commun. 59 (1990) 399.
[43] J.M. Longo, P.M. Raccah, Structure of La_2CuO_4 and $LaSrVO_4$, J. Solid State Chem. 6 (1973) 526.
[44] O.K. Anderson, Linear methods in band theory, Phys. Rev. B 12 (1975) 3060.
[45] O.A.O. Gunnarsson, O. Jepsen, Self-consistent impurity calculations in the atomic-spheres approximation, Phys. Rev. B 27 (1983) 7144. http://dx.doi.org/10.1103/PhysRevB.27.7144.
[46] O.J.O.K. Andersen, Explicit, first-principles tight-binding theory, Phys. Rev. Lett. 53 (1984) 2571. http://dx.doi.org/10.1103/PhysRevLett.53.2571.
[47] C. Ambrosch-Draxl, H. Auer, R. Kouba, E.Y. Sherman, P. Knoll, M. Mayer, Raman scattering in $YBa_2Cu_3O_7$: a comprehensive theoretical study in comparison with experiments, Phys. Rev. B 65 (2002) 064501. http://dx.doi.org/10.1103/PhysRevB.65.064501.
[48] C.-Z. Wang, R. Yu, H. Krakauer, First-principles calculations of phonon dispersion and lattice dynamics in La_2CuO_4, Phys. Rev. B 59 (1999) 9278.
[49] D.J. Singh, Phonons in La_2CuO_4: local density calculations, Solid State Commun. 98 (1996) 575.
[50] R.E. Cohen, W.E. Pickett, H. Krakauer, First-principles phonon calculations for La_2CuO_4, Phys. Rev. Lett. 62 (1989) 831.
[51] L. Pintschovius, N. Pyka, W. Reichardt, A. Yu Rumiantsev, N.L. Mitrofanov, A.S. Ivanov, G. Collin, P. Bourges, Lattice dynamical studies of HTSC materials, Phys. C 184 (1991) 156–161, http://dx.doi.org/10.1016/0921-4534(91)91965-7.
[52] G. Burns, F.H. Dacol, Anomalous raman spectra from La_2CuO_4, Phys. Rev. B 41 (1990) 4747.
[53] R. Henn, A. Wittlin, M. Cardona, S. Uchida, Dynamics of the c-polarized infrared-active modes in $La_{2-x}Sr_xCuO_4$, Phys. Rev. B 56 (1997) 6295.
[54] R.T. Collins, Z. Schlesinger, G.V. Chrashekhar, M.W. Shafer, Infrared study of anisotropy in single-crystal $La_{2-x}Sr_xCuO_4$, Phys. Rev. B 39 (1989) 2251.
[55] R. Kouba, C. Ambrosch-Draxl, B. Zangger, Structure optimization of $YBa_2Cu_3O_7$ and its influence on phonons and fermi surface, Phys. Rev. Lett. 60 (1999) 9321. http://dx.doi.org/10.1103/PhysRevB.60.9321.
[56] J. Spitaler, E.Y. Sherman, C. Ambrosch-Draxl, Zone-center phonons in NaV_2O_5: a comprehensive *ab initio* study including Raman spectra and electron–phonon interaction, Phys. Rev. B 75 (2007) 014302.
[57] C. Falter, M. Klenner, G. Hoffmann, Origin of phonon anomalies in La_2CuO_4, Phys. Rev. B 55 (1997) 3308. http://dx.doi.org/10.1103/PhysRevB.55.3308.
[58] N. Gedik, D.-S. Yang, G. Logvenov, I. Bozovic, A. Zewail, Non-equilibrium phase transitions in cuprates observed by ultrafast electron crystallography, Science 316 (2007) 425–429, http://dx.doi.org/10.1126/science.1138834.
[59] A. Macridin, B. Moritz, M. Jarrell, T. Maier, Suppression of superconductivity in the hubbard model by buckling and breathing phonons, J. Phys. Condens. Matter 24 (2012) 475603, http://dx.doi.org/10.1088/0953-8984/24/47/475603.
[60] G. Sangiovanni, O. Gunnarsson, E. Koch, Electron–phonon interaction and antiferromagnetic correlations, Phys. Rev. Lett. 97 (2006) 046404. http://dx.doi.org/10.1103/PhysRevLett.97.046404.